Molecular Therapy
Nucleic Acids
Original Article

Understanding the biological limits of hybridization-dependent siRNA off-target interactions

Luca Penso-Dolfin,[1,2] Judith Hauptmann,[1,2] Nina Was,[1] Vivien Hehne,[1] Marie Wikström Lindholm,[1] and Eliot Morrison[1]

[1]Silence Therapeutics GmbH, Robert-Rössle-Str. 10, 13125 Berlin, Germany

Understanding off-target risk is a key element of siRNA design, but predicting hybridization-dependent off targets using *in-silico* alignments is limited by an incomplete understanding of when and how low-homology and seed-mediated off targets lead to functional downregulation. Here we explore the biological limits of these interactions by measuring the off-target profiles of six "promiscuous" siRNAs with intentional off targets on both an mRNA and protein level, using a cell system featuring catalytically inactive Argonaute 2 (Ago2) to distinguish cleavage-dependent and -independent mechanisms of downregulation. By probing the *in-silico* alignments of the observed off targets with the siRNA sequences, several intriguing patterns emerge; multiple G:U wobbles and target bulges, for example, are more frequently seen than bulges in the siRNA guide strand. Further, a clear sequence-dependence is observed for the overall extent of cleavage-independent downregulation of off targets; this may be explained by impaired unwinding and loading of the fully ribose-modified siRNA into RNA-induced silencing complex (RISC), suggesting an additional nuance to seed-mediated off-target risk associated with other Argonaute proteins. Taken together, this study sheds new light on potential siRNA off-target risk and may help guide and improve the *in-silico* prediction of siRNA:off-target interactions.

INTRODUCTION

Small interfering RNAs (siRNAs) are a class of oligonucleotide therapeutics that act to downregulate target mRNA expression in a highly specific manner. After loading the siRNA duplex into an Argonaute (Ago) protein, the passenger strand is cleaved by Ago2, facilitating its removal and the maturation of a Ago2-RISC (RNA-induced silencing complex) complex loaded with the guide (antisense) strand, which targets specific sites on mRNA transcripts via sequence complementarity. Extensive guide: target complementarity is a prerequisite for endonucleolytic cleavage of the target by Ago2, the only Ago protein with efficient slicer activity by small RNAs of ~20 nt length.[1] However, this mechanism can tolerate some imperfect complementarity,[2,3] leading to the potential for off-target (OffT) effects driven by a lower degree of sequence similarity. The seed region, positions g2-g7 of the guide strand (5′>3′), is well-established as a feature where sequence complementarity is critical for miRNA-mediated target degradation and translational repression.[2–5] Although it has been shown that seed complementarity alone is not sufficient for target repression, the exact nature of imperfect seed complementarity tolerance in the context of siRNA OffTs is still unclear.[6]

To minimize such hybridization-dependent OffT risk when designing therapeutic siRNAs, alignment-based approaches have been developed to identify potential siRNA OffT target activity with imperfect sequence complementarity between the siRNA guide strand and the OffT mRNA.[7,8] Such hybridization-dependent OffTs are generally considered to belong to one of two classes: those with a high degree of sequence similarity that are cleaved and downregulated via an siRNA-like mechanism, and those with overall low similarity but high complementarity in the seed region, which may act to repress mRNA translation in a manner similar to that of endogenous miRNAs—that is, base-pairing with complementary sequences on the target mRNA, blocking ribosomal initiation and elongation, and repressing translation.[3,7–9] When searching for the former category using *in-silico* alignment methods, a high degree of sequence similarity is defined *a priori*, resulting in a limited number of OffT alignments in the target species transcriptome due to the low probability of a highly similar sequence match. For this reason, predicting such OffTs *in silico* is relatively straightforward with a low risk of false positives. The latter category, however, suffers from an especially high false positive rate (i.e., many seed alignments identified *in silico* do not result in observable OffT downregulation) when alignment alone is performed.[8] For all OffT alignment strategies, a limited understanding of the biological mechanisms of potential low-homology and seed-mediated OffT interactions means that *in-silico* predictions are often run with highly permissive alignment

Received 9 December 2025; accepted 29 May 2026;
https://doi.org/10.1016/j.omtn.2026.102972.

[2]These authors contributed equally

Correspondence: Eliot Morrison, Silence Therapeutics GmbH, Robert-Rössle-Str. 10, 13125 Berlin, Germany.
E-mail: e.morrison@silence-therapeutics.com

settings—that is, allowing for multiple mismatches, insertions, and/or deletions. This is followed by experimental screening using a method like RNA sequencing (RNA-seq), a strategy that is effective at identifying hybridization-dependent OffT risk but resource-intensive when performed at larger scales.[10,11]

Here we sought to investigate the biological limits of hybridization-dependent OffT downregulation with the aim of improving our understanding of the underlying mechanisms driving these interactions and to better inform *in-silico* OffT prediction methods. We first designed siRNA sequences that were intentionally promiscuous (i.e., with many predicted OffTs featuring a range of sequence complementarity) and measured their OffT profiles on both an mRNA and protein level using RNA-seq and label-free proteomics methods, respectively. Both methods are untargeted (i.e., potential OffTs are not defined *a priori*) and so are relatively unbiased, capturing global changes on a transcript and protein level, respectively. We further developed a cellular system expressing endogenous Ago2 edited to be catalytically inactive, allowing us to probe global OffT profile changes and differentiate between cleavage-dependent (i.e., siRNA-like) and cleavage-independent (i.e., miRNA-like) mechanisms. It should be noted that the cleavage described here refers to the Ago2-mediated cleavage of target mRNA, not the cleavage of the passenger strand during Ago2-RISC maturation. A comparable approach has previously been reported with SpyCLIP, where a tagged, stably overexpressed Ago2 mutant was used to identify both cleavage-dependent and -independent interactions.[12] The latter approach used unmodified siRNAs, whereas the current study uses 2′-OMe ((2′-O-methyl) and 2′-F-modified siRNAs with phosphorothioate (ps) modifications for end stabilization. Unexpectedly, among the siRNAs tested in the current study two classes emerged: those whose overall activity was reduced in the mutant Ago2 cell line and those who retained some cleavage-independent activity; we hypothesize this difference may relate to differentially impaired passenger strand cleavage, and therefore unwinding and loading, of the siRNA duplex.

Performing *in-silico* alignment of all identified OffTs with the tested siRNAs allowed us to identify alignment features that were surprisingly compatible with OffT downregulation, such as large target bulges (i.e., insertions in the mRNA target site). Using a luciferase-based reporter system, we were able to validate and generalize several selected OffT target site patterns experimentally. Taken together, these results suggest several specific ways that the *in-silico* prediction of potential siRNA OffTs may be extended to help improve predictive power without unduly increasing the false positive rate.

RESULTS

Establishing a catalytically inactive Ago2 cellular system

Performing untargeted RNA-seq or proteomics on cells treated with a promiscuous siRNA will result in the detection of a combination of genes downregulated by both siRNA-like and miRNA-like mechanisms. To disentangle these effects, we sought to establish a cellular system capable of downregulating via only the latter of these two mechanisms. It has been previously reported that the D597A mutation of Ago2 is catalytically inactive and is incapable of downregulating targets via slicing.[13] By using CRISPR/Cas9 to mutate endogenous Ago2, we aimed to generate a stable cell line capable of only miRNA-like target repression (Figure 1A). We chose an editing approach instead of an Ago2 knockout because Ago2 contributes a major part to the total pool of Ago proteins[14] and we wanted to avoid introducing additional bias by changing relative Ago protein levels in our system.[15,16]

Although siRNAs are widely used conjugated to hepatocyte-targeting GalNAc sugars, hepatic cell lines are not viable upon loss of Ago2 slicing function.[17] We therefore chose the A549 cell line, a human line derived from alveolar basal epithelial cells originating from cancerous lung tissue, for editing. Protein levels of Ago1, Ago2, and Ago3 have been demonstrated to be comparable in whole lung and liver tissue.[14] To ensure that only the edited endonuclease is expressed in this system, we performed genotyping of the Ago2 locus in the Ago2 D597A-expressing cells (Figure S1); two point mutations were observed: the intended D597A mutation, and a silent TTT>TTC mutation that leaves Phe593 unchanged.

To test if slicing activity was impaired in the Ago2 D597A-expressing cell line, six siRNAs targeting peptidylprolyl isomerase B (PPIB) were transfected at 20 nM in wild-type (WT) and Ago2 D597A-expressing cells (Figure 1B). PPIB was selected as a tool target for several reasons, including its stable and ubiquitous expression in many cell types, its amenability to knockdown via siRNA downregulation, and the existence of well-established quantification methods like quantitative reverse-transcription PCR (RT-qPCR). All six siRNAs showed robust (>95%) downregulation of the target in the WT cells, which was impaired in the Ago2 D597A-expressing cells. Interestingly, for one of the six tested siRNAs (siRNA-3), some degree of target downregulation was achieved in the Ago2 D597A-expressing cell line, possibly suggesting a combined cleavage-dependent and -independent mechanism for this specific siRNA.

To confirm that miRNA-like activity was retained in the Ago2 D597A-expressing cells, two strategies were used: first, two luciferase-based reporter systems were designed to probe activity either on full-match siRNA target sites (19-nt in length; “siRNA reporter”) or seed-mediated activity (multiple seed sites complementary to positions 2–8 of the antisense; “miRNA reporter”). Our expectation was that siRNAs in the Ago2 D597A-expressing cell line would show impaired activity in the siRNA reporter but retained activity in the miRNA reporter system. A GalNAc-siRNA conjugate targeting transthyretin (TTR) was co-transfected with both reporters (Figure 1C). For the fully complementary siRNA target site, activity was dramatically impaired (but not completely absent) in the Ago2 D597A-expressing cells, while WT cells showed robust downregulation (Figure 1C). Unexpectedly, seed-mediated activity was also impaired in the Ago2 D597A-expressing cells using this reporter system. The observation was confirmed with a second sequence

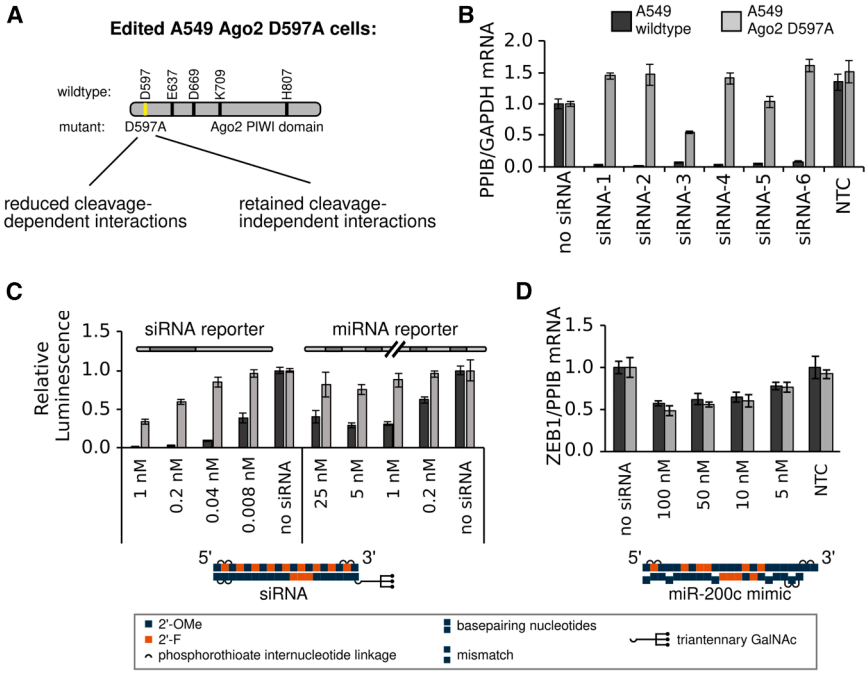

Figure 1. Characterization of a cell system with catalytically inactive Ago2

(A) D597 was edited to A597, which is known to eliminate endonucleolytic activity and expected to retain function in seed-mediated target repression. (B) On-target activity was reduced in A549 mutant cells as compared to WT cells, as confirmed by transfection of six sequences targeting PPIB and analysis of target gene levels by RT-qPCR. (C) Seed-mediated off-target activity was reduced in A549 mutant as compared to WT cells, as demonstrated with a luciferase reporter system containing multiple seed target sites and a perfectly complementary, fully 2′-OMe/2′-F-modified GalNAc siRNA conjugate. (D) miRNA-mediated target reduction of the endogenous miR-200c target ZEB1 was at equal levels in A549 mutant and WT cells, as demonstrated by transfection with a 2′-OMe/2′-F-modified miRNA mimic and RT-qPCR readout of target level. (E) Schematic illustrating possible failure in RISC maturation and target cleavage in Ago2 D597E-expressing cells.

targeting aldehyde dehydrogenase 2 (ALDH2) (Figure S2A) and also after elongating siRNA treatment from 24 to 48 h (Figure S2B).

As we did not observe the expected retained seed-mediated activity with fully ribose-modified, fully complementary siRNA duplexes, we sought to confirm retained miRNA-like activity by the use of miRNA mimics targeting endogenously expressed ZEB1 and ZEB2.[18] In both WT and Ago2 D597A-expressing cells, downregulation of ZEB1 (Figure 1D) and ZEB2 (Figure S3) was observed, supporting the conclusion that the cell line expressing catalytically inactive Ago2 has retained seed-mediated target repression activity while abolishing cleavage-dependent siRNA-based target downregulation. Unlike the siRNAs tested, these fully ribose-modified miRNA mimics feature multiple mismatches between the two strands of the duplex (Figure 1D); we hypothesized that the lower duplex thermal stability may assist duplex unwinding and the formation of the active Ago2/RISC complex.

One explanation for this observation is that catalytically inactive Ago2 affects siRNA maturation (the multi-step process of loading the siRNA guide strand into Ago2/RISC) at the stage of passenger strand cleavage, and the "bypass mechanism" of cleavage-independent unwinding may be impeded in fully complementary siRNA duplexes with extensive 2′-OMe and 2′-F ribose modifications that increase duplex melting temperature (T_m) substantially (Figure 1E).[19–21] To evaluate this possibility, we transfected WT and Ago2 D597A-expressing cells with an siRNA targeting TTR, immunoprecipitated Ago2, and quantified Ago2-associated guide and passenger strands by stem-loop RT-qPCR. While associated with comparable amounts of guide strand, the passenger/guide ratio was higher in Ago2 D597A-expressing cells (38%) as compared to WT cells (22%), supporting compromised passenger strand removal (Figure S4).

Furthermore, we revisited on-target activity of the six sequences tested (Figure 1B) and measured T_m values of the siRNA duplexes (Table S2). Although siRNA-3 reduces the target most in A549 mutant cells, it is not characterized by the lowest duplex T_m of the six duplexes tested. It is clear that the T_m of the full duplex does not fully explain the observed sequence-dependent reduction in OffT activity; other factors, including local interactions of the two strands in specific regions of the duplex, differential duplex opening dynamics, or accessibility of target sites may contribute to the overall functionality in the catalytically inactive Ago2 system.

In the following experiments we compared data from the WT and the Ago2 D597A-expressing cellular system described previously to classify the downregulation of all observed OffTs as either "cleavage-dependent" (i.e., downregulation is seen in the WT cell line but not the catalytically inactive Ago2 cell line) or "cleavage-

independent" (i.e., downregulation is seen in both cell lines, suggesting a seed-mediated target repression mechanism).

Cleavage-dependent unwinding of siRNA duplexes contributes to seed-mediated activity in catalytically inactive argonaute proteins

To better understand to what extent different siRNA sequences rely on passenger strand cleavage, we tested four sequences targeting PPIB with the previously described siRNA and miRNA reporters (Figure S5). All sequences demonstrated reduced siRNA-mediated activity in the Ago2 D597A-expressing cells. In WT cells, siRNA-1 barely reduced the miRNA reporter readout, whereas siRNA-3, -4, and -6 reduced reporter readout. However, the readout in the Ago2 D597A-expressing cells varied between retained miRNA activity (siRNA-1 and siRNA-3) and reduced miRNA activity (siRNA-4 and siRNA-6). We conclude that seed-mediated target reduction can be affected in a sequence-dependent manner in cells with catalytically inactive Ago2.

Global transcript-level OffT profiles of promiscuous siRNAs by RNA-seq

To probe global OffT interactions in a cellular context, six siRNAs targeting PPIB were designed *in silico* to be intentionally promiscuous (i.e., feature multiple hybridization-dependent OffTs) while still retaining a high degree of on-target downregulation activity. We chose the ubiquitously expressed target PPIB as a tool target gene and, using alignment-based OffT prediction software, designed 19-mer siRNAs with multiple predicted OffTs (Table S1). We aimed to find sequences with OffTs alignments with a wide range of complementarity, from fully complementary alignments (e.g., siRNA-4 and CIAO2A), nearly fully complementary alignments (e.g., siRNA-6 and HUNK), and alignments with overall low complementary but with perfect seed matches in the OffT mRNA (e.g., siRNA-2 and SKAP2); the total number of predicted OffTs numbered at least several hundred per sequence, depending on the complementarity threshold used. These aligned OffT genes were cross-referenced with publicly available expression data to ensure adequate expression in WT A549 cells (Human Protein Atlas, accessed: 10.2023).

On-target activity of the promiscuous siRNAs described previously was confirmed by transfection into WT A549 cells and, after this, both WT and catalytically inactive Ago2 D597A-expressing cell lines were treated with the promiscuous siRNAs by transfection at 20 nM for 24 h (Figure 1B). A non-targeting control (NTC) siRNA with the same chemical modifications as the promiscuous siRNAs and designed to downregulate luciferase was used to control potential effects arising from the transfection method and presence of siRNA itself. Following treatment, isolated RNA was sequenced by RNA-seq and differential gene expression (DGE) analysis was performed comparing each treated sample to the cell samples treated with the NTC; all fold-change values mentioned in this study refer to the comparison between cells treated with the promiscuous siRNAs and the NTC siRNA (Figure 2).

As anticipated, a large number of differentially expressed genes (DEGs), including the on-target PPIB, were observed following treatment with all six siRNAs tested in the Ago2 WT-expressing cell line as measured by RNA-seq. Beyond the on-target PPIB, some measured OffTs show very strong (log2(fold change) < −3.0) significant downregulation following siRNA treatment; these include FKBP2, LIMS1, and USP38 for siRNA-1; PPI family members, and related pseudogenes PPIA, PPID, PPIAP22, PPIAP29, and PPIAP31 for siRNA-4; and CXCL5, RAP2A, and MOB1A for siRNA-2. A handful of DEGs were also observed to be strongly upregulated (log2(fold change) > 3.0) upon siRNA treatment; these include XAGE1B and F13B for siRNA-1 and SMIM1 for both siRNA-2 and siRNA-5. The direct upregulation of an OffT via siRNA is unlikely given the mechanism by which Ago2/RISC-mediated mRNA regulation occurs; however, secondary and downstream effects of other direct OffTs may explain these observed upregulated DEGs and could form the basis for future systems biology studies. In the Ago2 D597A-expressing cell line, four of the six tested siRNAs showed a loss of nearly all identified DEGs, including the on-target PPIB. siRNA-2 and siRNA-3, however, showed some retained OffT activity. Further, siRNA-3 also retained on-target activity, albeit attenuated (Ago2 WT log2(fold change) = −4.42, Ago2 D597A log2(fold change) = −2.35). This is in agreement with downregulation activity of PPIB as measured by RT-qPCR (Figure 1B).

Global protein-level OffT profiles of promiscuous siRNAs by label-free proteomics

After identifying transcript-level DEGs by RNA-seq for the six promiscuous siRNAs, we then explored how such changes translate to differential protein-level expression using label-free proteomics. Of special interest are potential OffTs driven by seed-mediated translational repression; here, protein-level downregulation may be more exaggerated than mRNA-level decreases.[22] To account for a potentially slower onset of effects at the protein level due to protein turnover rates, we assayed PPIB protein reduction after 1–4 days by western blot and, based on this, chose an incubation time of 48 h (Figures S6A and S6B). We validated PPIB mRNA reduction after 48 h (Figure S6C), which was in line with target mRNA downregulation after 24 h (Figure 1B).

When measured on a protein level, significantly downregulated (fold-change < 0.5, adjusted q value < 0.05) differentially expressed proteins were seen for the Ago2 WT-expressing cell line treated with all six siRNAs, albeit at lower numbers than seen by RNA-seq (Figure 3). All six siRNAs showed significant protein-level knockdown of the on-target PPIB. The numbers of differentially downregulated proteins seen in the Ago2 D597A-expressing cell line were dramatically reduced, with the exception of siRNA-2 and siRNA-3, where a small number were retained. Intriguingly, in the Ago2 WT-expressing cells, many proteins are also seen to be significantly upregulated. While knocking down endogenous miRNAs can lead to upregulation of protein targets[22] the mechanism by which a promiscuous siRNA may drive such a change is less clear.

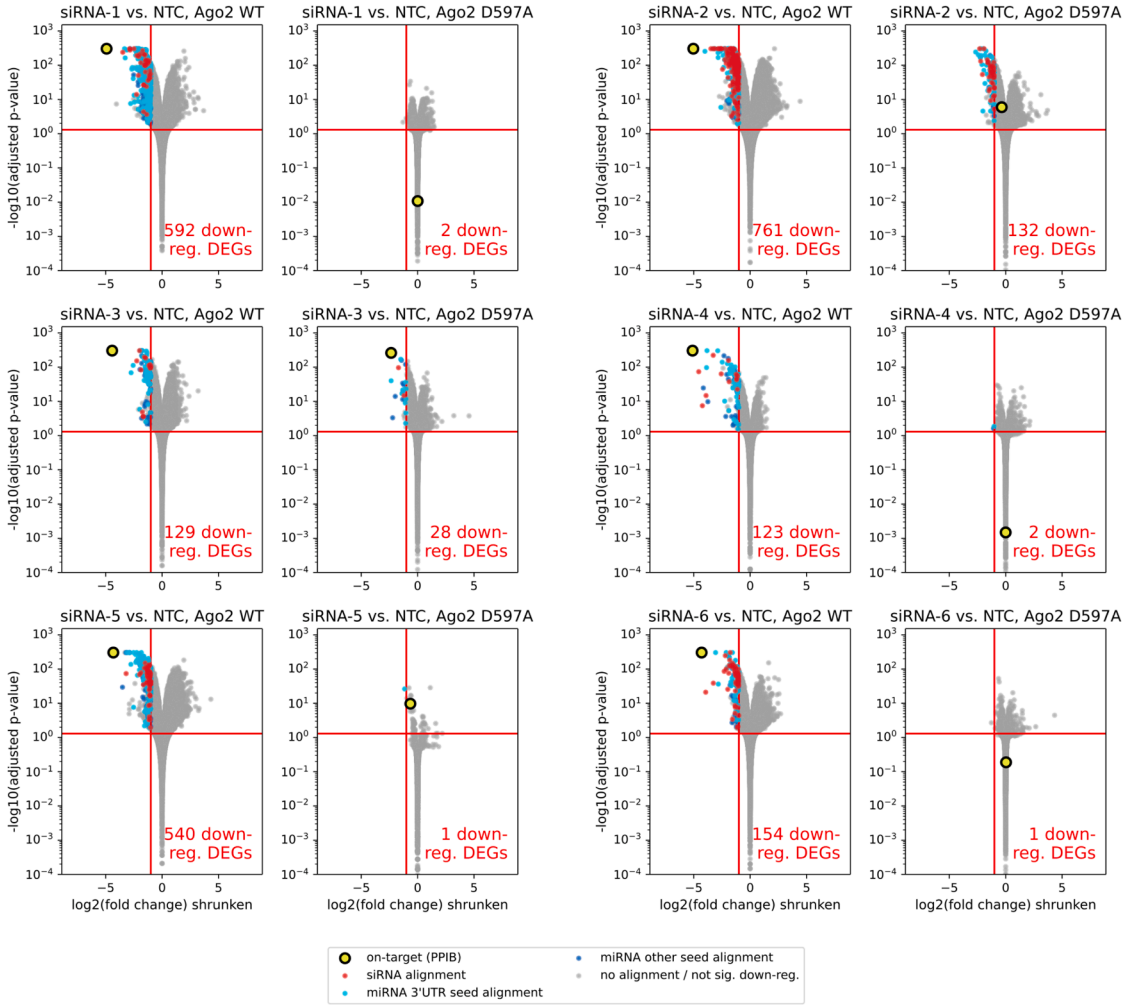

Figure 2. Volcano plots showing differential gene expression of WT (left) and D597A Ago2 (right) A549 cells treated with six different siRNAs relative to treatment of luciferase non-targeting control (NTC) measured by RNA-seq

All siRNAs were transfected at 20 nM for 24 h Differential expression was calculated by comparing samples treated with promiscuous siRNAs to those treated with the NTC siRNA. Genes were considered significantly downregulated when the fold-change was ≤ 0.5 ($\geq 50\%$ downregulation) and the adjusted p value was ≤ 0.05 (upper-left quadrant, red lines). The on-target (PPIB) is highlighted. Significantly downregulated genes are colored based on the IntaRNA alignment of the siRNA and the canonical transcript mRNA: red: siRNA-like alignment; light blue: 3′-UTR seed match; dark blue: non-3′-UTR seed match.

The proteomics data generated here also allow us to validate that the CRISPR/Cas9-based editing of Ago2 did not affect the relative levels of the different Ago proteins (Table S3).

Comparing siRNA: OffT profiles identified by RNA-seq and label-free proteomics

To understand the translatability of identified OffT effects by RNA-seq to those seen on a protein level, we performed a systematic comparison of the two datasets (Figure 4A). For all six siRNAs tested in Ago2 WT-expressing cells, a handful of OffTs were found at both an mRNA and protein level (Figure 4A, lower-left quadrant), while the majority of OffTs were seen only by RNA-seq (Figure 4A, upper-left quadrant). For Ago2 D597A-expressing cells, the two siRNAs with some degree of retained OffT activity (siRNA-2 and siRNA-3) showed a similar pattern, with the majority of OffTs observed only by RNA-seq. Interestingly, our expectation that the Ago2 D597A-expressing cell system would show an over-representation of differentially expressed proteins due to retained miRNA-like translational suppression was not supported, even for siRNA-2 and siRNA-3, where cleavage-dependent loading may be less impaired. This may be partially explained by a temporal lag phase for OffT proteins with extended half-lives, whose downregulation may be seen at an mRNA level by 24 h but not at a protein level until after 48 h.[22]

The degree of downregulation of the on-target PPIB at both mRNA and protein levels is largely in agreement in both Ago2 WT- and

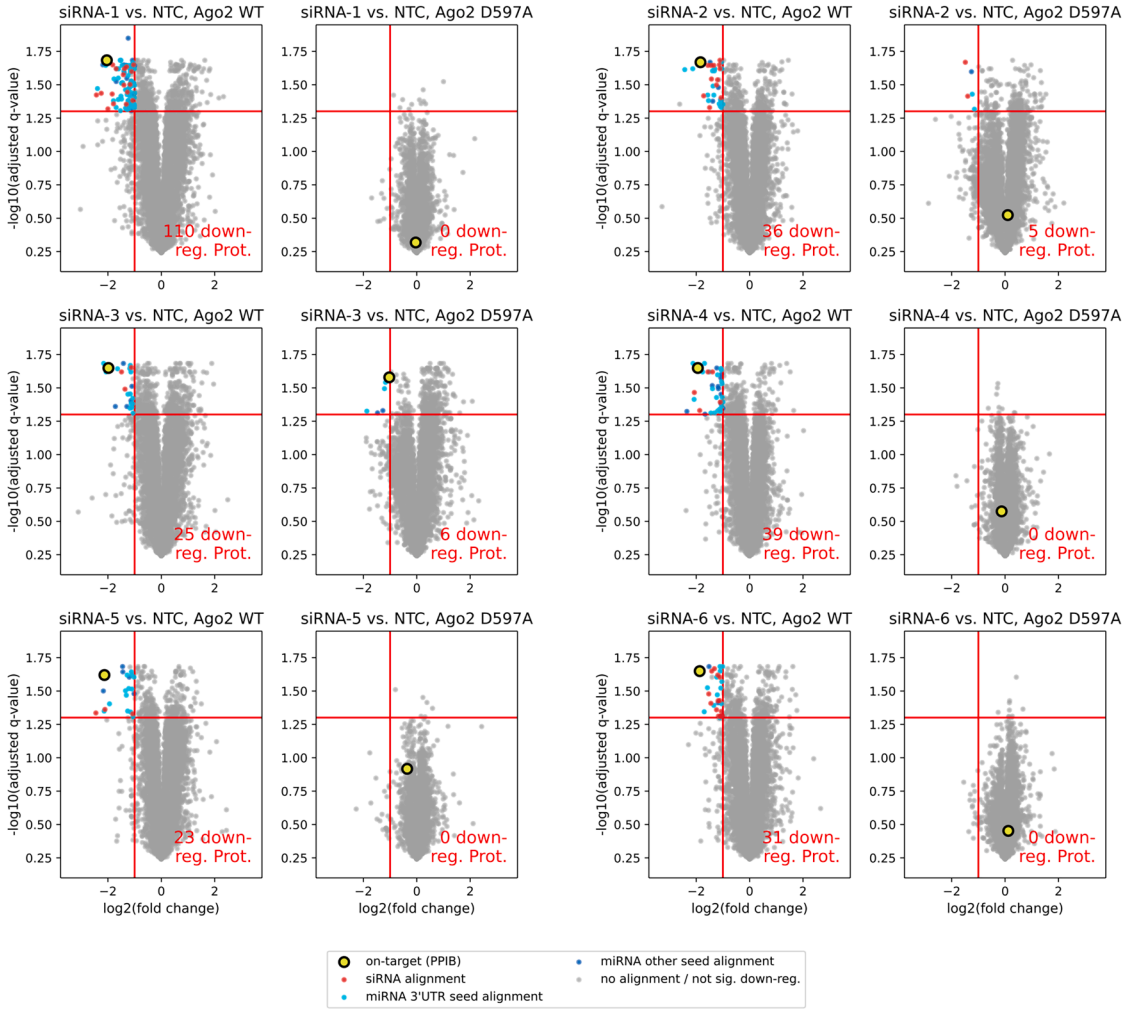

Figure 3. Volcano plots showing differential protein expression of WT (left) and D597A Ago2 (right) A549 cells treated with six different siRNAs relative to treatment of luciferase non-targeting control (NTC) measured by label-free proteomics

All siRNAs were transfected at 20 nM for 48 h. Differential expression was calculated by comparing samples treated with promiscuous siRNAs to those treated with the NTC siRNA. Proteins were considered significantly downregulated when the fold-change was ≤ 0.5 ($\geq 50\%$ downregulation) and the adjusted p value was ≤ 0.05 (upper-left quadrant, red lines). The on-target (PPIB) is highlighted. Significantly downregulated proteins are colored based on the IntaRNA alignment of the siRNA and the canonical transcript mRNA: red: siRNA-like alignment; light blue: 3′-UTR seed match; dark blue: non-3′-UTR seed match.

Ago2 D597A-expressing cell systems and across all tested methods: RNA-seq (Figures 2 and 4A), RT-qPCR (Figure 1B), western blotting (Figure S6A), and label-free proteomics (Figures 3 and 4A).

Comparing siRNA:OffT profiles in Ago2 WT- and Ago2 D597A-expressing cell lines

To further characterize the identified OffTs, we sought to categorize them into those regulated by an Ago2 cleavage-dependent and a cleavage-independent mechanism (Figure 4B), both at mRNA and protein level. By both methods, we identified a sequence-dependent effect: four of the six siRNAs tested have OffT profiles entirely cleavage-dependent (Figure 4B, upper left quadrant), while two siRNAs have some retained OffT activity in a cleavage-independent manner (Figure 4B, lower left quadrant). This trend is observed on both an mRNA and protein level, although the overall numbers of differentially expressed proteins are lower than the numbers of RNA-seq-identified DEGs in all cases.

Interestingly, for the two siRNAs with retained cleavage-independent OffT activity, the cleavage-independent DEGs are a mix of both siRNA-like alignments (see alignment and in-silico characterization of identified siRNA: OffT target site interactions) and those with perfect seed matches (Figures 2 and 4B). We originally hypothesized that cleavage-independent OffTs would be predominantly driven by seed matches; however, many (190/231) of the cleavage-independent siRNA-like alignments also feature perfect

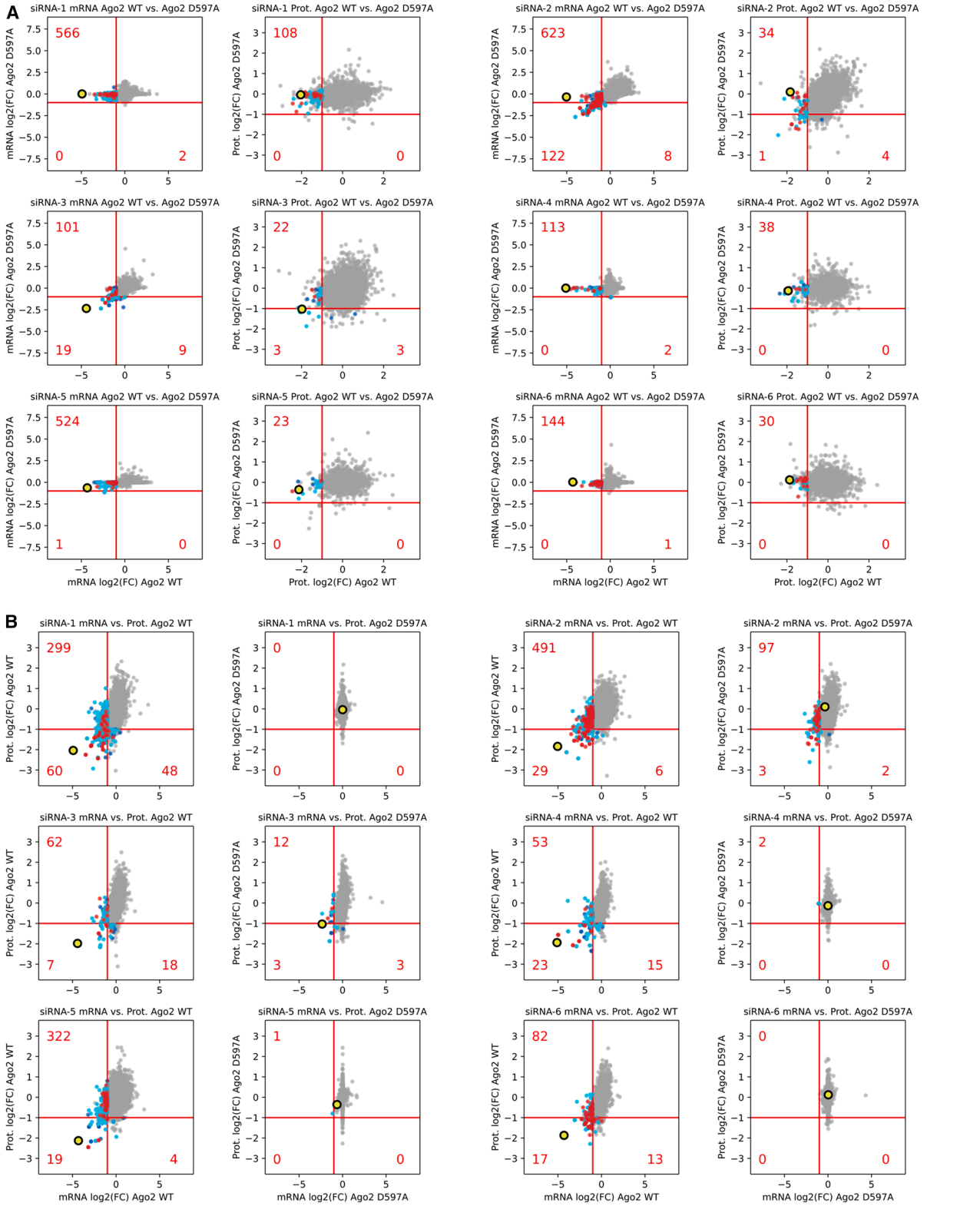

(legend on next page)

seed matches in the 3′UTR, suggesting the possibility of an alternative or combined cleavage-independent mechanism.

Alignment and *in-silico* characterization of identified siRNA: OffT target site interactions

After experimentally identifying the OffT profiles of the six tested siRNAs and characterizing their Ago2 cleavage dependence using the catalytically inactive Ago2 D597A-expressing cell line, we next sought to understand the nature of the biological mechanism further through *in-silico* characterization of the siRNA:target site interactions. All siRNA:OffT pairs identified by RNA-seq were aligned to each other using the RNA-RNA interaction prediction software IntaRNA.[23–26] In cases where multiple alignments were identified, the "best" alignment was defined as that having the lowest (most negative) interaction energy.

We then categorized all *in-silico* alignments using a hierarchical approach: first, any alignment with fewer than three mismatches (excluding G:U wobbles) or bulges in the region between positions g2 and g18 of the siRNA guide strand, a match at g10 and g11, and an interaction energy < -15 kcal/mol was classified as an "siRNA-like" alignment.[5,27,28] Alignments not meeting these criteria were then checked for perfect seed matches in the 3′UTR (category "miRNA 3′UTR"). If no 3′UTR seed match was found, other regions of the target mRNA were checked for perfect seed matches (category "miRNA other"), as such target sites in the 5′UTR and coding regions have been identified as active miRNA target sites.[29,30] Alignments not meeting any of these criteria were classified as "hybridization-independent"; these may be downregulated via an alternative mechanism (e.g., secondary effects, pathway effects, and/or artifacts of the experimental method).

Note that the alignment classifications introduced here are hierarchical and mutually exclusive: an alignment classified as siRNA-like, for example, may also feature a 3′UTR seed match and so may be downregulated via multiple mechanisms.

A comprehensive *in-silico* analysis of all identified significantly downregulated DEGs of all six pooled siRNAs in Ago2 WT-expressing cells was performed to identify features apparently compatible with endogenous siRNA OffTs (Figure 5). As a point of comparison, 13,137 endogenous human miRNA:target pairs reported as functional in MiRTarBase were aligned using the same approach.[31–33] By comparing the alignments performed on the DEGs observed in this study with validated miRNA:target alignments, we hoped to define the range of alignment features generally compatible with RISC-mediated downregulation in the context of endogenous miRNA activity.

Four different alignment features were characterized: mismatches, G:U wobbles, target bulges (an insertion in the aligned target sequence), and guide bulges (an insertion in the aligned guide sequence).[3] For all features, the position on the guide strand (5′>3′), the total number found in each alignment, and, for the bulges, the size of the insertions, were analyzed.

Validation and generalization of novel siRNA:OffT interactions by luciferase reporter system

The global transcript- and protein-level OffT profiles of the six tested siRNAs revealed some intriguing and unexpected potential mRNA OffTs. Further, when analyzed globally, alignment features normally deprioritized during *in-silico* OffT prediction alignments were found to be widely represented. From this analysis, we selected two unexpected features for extended experimental validation (Figure 6). First, we wanted to investigate the apparent tolerance for large target bulges, even at positions near the cleavage site; to test this, we forced a 5-nt target bulge at position g9 (represented in alignments such as siRNA-6/FGG (Figure S7). Second, using the alignment of siRNA-4/FXR1 as exemplary (Figure S7), we wanted to explore the apparent tolerance of a mismatch at position g12, a position at which mismatches were previously reported to enhance the rate of Ago2 cleavage-dependent downregulation[5]

To validate and generalize these patterns to other potential siRNA:OffT interactions, we established a luciferase reporter system with ten target sites for ten new siRNA sequences, arranged in a serial "concatemeric" fashion (Table S1). We then edited these target sites to force the specific features described previously and tested the siRNA-mediated downregulation experimentally (Figure 6). After ensuring no inadvertent secondary target sites were introduced during editing using *in-silico* alignment, all ten tested siRNAs showed robust downregulation of the fully complementary reporter. All ten siRNAs also showed moderate downregulation of the 5-nt target bulge reporter, albeit to different degrees, supporting the hypothesis that large target bulges may be generally compatible with OffT activity, even in positions near the Ago2 cleavage site. For the edited reporter featuring the g12 mismatch, however, downregulation activity was more severely attenuated for most of the ten siRNAs tested, in contrast to the previous report suggesting mismatches at this position can enhance the rate of Ago2 cleavage activity[5] siRNA-4 also features a perfect seed match in the 3′UTR of FXR1's canonical transcript (ENST00000357559.9), suggesting an alternative mechanism

Figure 4. Comparison of transcript- and protein-level changes in WT and D597A Ago2-expressing A549 cells

(A) Comparison of log2(fold-change) on mRNA and protein levels in WT Ago2 (left) and D597A Ago2 (right) A549 cells treated with six siRNAs relative to treatment with the NTC siRNA. Numbers summarize number of significantly downregulated genes/proteins at both mRNA and protein levels (bottom left), mRNA only (upper left), and protein only (lower right). (B) Comparison of log2(fold-change) on mRNA (left) and protein (right) levels between WT Ago2 and D597A Ago2 A549 cells treated with six siRNAs relative to treatment with luciferase non-targeting control. Numbers summarize number of significantly downregulated genes/proteins in both WT and D597A Ago2 (bottom left), WT Ago2 only (upper left), and D597A Ago2 only (lower right). The on-target (PPIB) is highlighted. Significantly downregulated genes/proteins are colored based on the IntaRNA alignment of the siRNA and the canonical transcript mRNA, red, siRNA-like alignment; light blue, 3′-UTR seed match; dark blue, non-3′-UTR seed match.

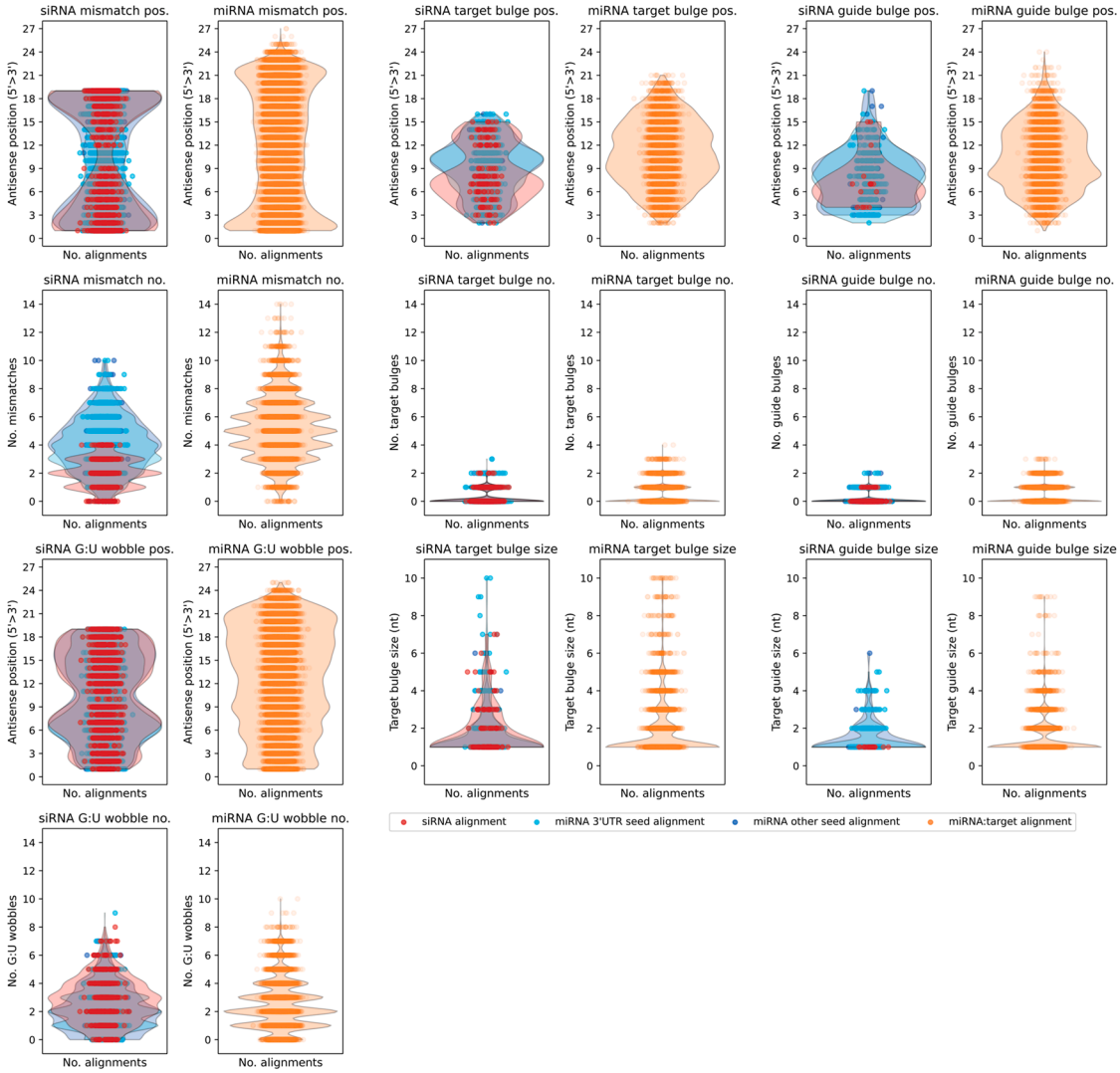

Figure 5. Summary of alignment features of pooled siRNA and miRNA alignments: significantly downregulated targets (RNA-seq, WT Ago2, fold-change ≤ 0.5, adjusted *p* value ≤ 0.05) identified in this study (blue and red) and in alignments between miRNA

target canonical transcript mRNA identified with a functional miRNA-target interaction by MiRTarBase (orange). Genes are colored based on the IntaRNA alignment of the siRNA and the canonical transcript mRNA, red, siRNA-like alignment; light blue, 3′-UTR seed match; dark blue, non-3′-UTR seed match. Upper row: position on antisense strand (5′>3′) of identified mismatches, target bulges, and guide bulges. Second row: distribution of total number of mismatches, target bulges, and guide bulges identified in each alignment. Third row: position on antisense strand (5′ > 3′) of identified G:U wobbles and distribution of size, in nucleotides, of target bulges and guide bulges identified in each alignment. Bottom row: distribution of total number of G:U wobbles identified in each alignment.

for the observed downregulation of this transcript in a cellular context by RNA-seq.

Effects of seed destabilization on identified siRNA:OffT interactions

To further validate the hybridization-dependent nature of the siRNA:OffT interactions identified in this study, we treated Ago2 WT cells with two siRNAs featuring seed-destabilizing chemical modifications (Figure 7). After performing a seed walk to identify a position with retained on-target activity (Figure S8), we incorporated single glycol nucleic acids (GNAs) in the seed of each siRNA at a position compatible with on-target activity (Figure S9). By destabilizing the seed:target site interaction, GNA has been shown to effectively reduce the downregulation of hybridization-dependent OffTs in siRNAs.[34]

In both siRNAs tested, the inclusion of GNA in the seed reduced the number of significantly downregulated DEGs identified by RNA-seq while retaining on-target activity (Figure 7; Figure S10). Neither siRNA, however, showed a complete loss OffT activity, with the

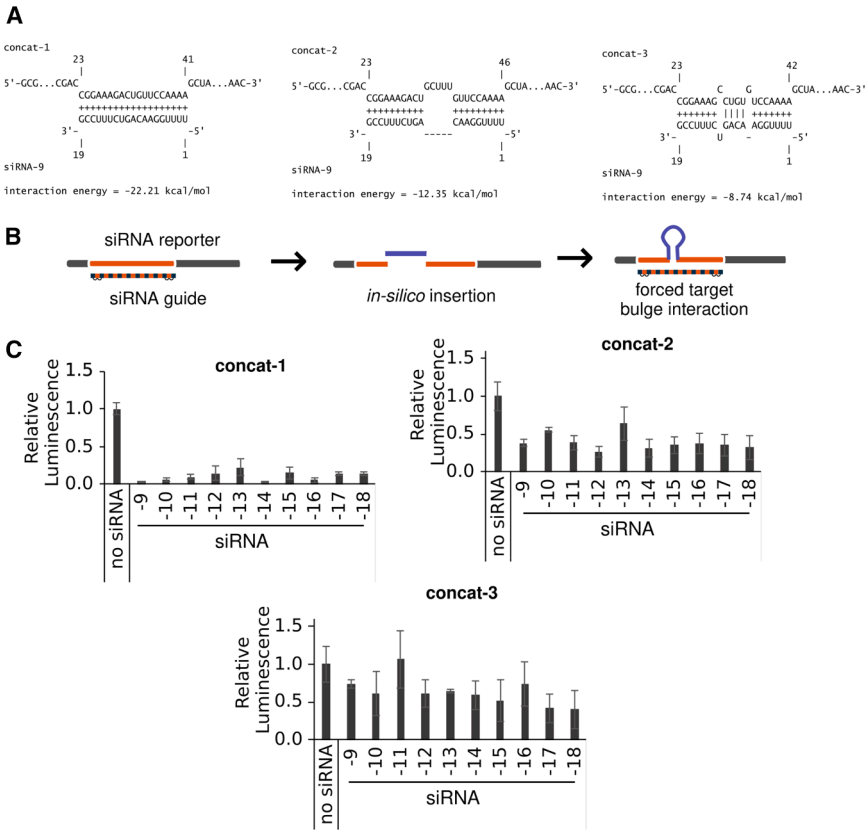

Figure 6. Validation and generalization of two siRNA:OffT features by concatemeric luciferase reporter system

(A) Representative IntaRNA alignments of siRNA-9 with the fully complementary (concat-1) and two edited reporter sequences (concat-2 and concat-3). (B) Schematic illustrating the *in-silico* generation of edited reporters, forcing the desired siRNA:reporter interaction. (C) Relative luminescence of three reporters treated with ten different siRNAs after 24 h incubation.

seed-destabilized siRNA-2 retaining more than 600 DEGs (vs. 761 DEGs of the reference molecule). Approximately 56%–67% of the DEGs negatively affected by seed destabilization feature a perfect seed match in the 3′UTR of the OffT mRNA transcript vs. approximately 10%–32% with an siRNA-like alignment. Of the DEGs with retained downregulation using seed destabilization, a similar distribution of alignments is seen: approximately 14%–24% feature an siRNA-like alignment and 49%–66% have a perfect seed match in the 3′UTR, suggesting that the nature of the siRNA:OffT alignment alone does not explain the DEGs observed using seed destabilization. The observation of a high number of DEGs following treatment with seed-destabilized siRNAs was unexpected; a possible explanation may be the existence of secondary OffT effects—that is, a direct downregulation of a "high-impact" OffT (e.g., a transcription factor) resulting in many secondary OffT downregulation effects.

The GNA-dependent attenuation of downregulation activity was further validated for four of the DEGs observed by RNA-seq using RT-qPCR (Figure S10). This reduction of the OffT profiles by inclusion of the seed-destabilizing chemistry validates the conclusion that some, if not all, of the DEGs in this study are directly or indirectly driven by hybridization-dependent siRNA:OffT interactions, although the retained DEGs may be driven by an alternative mechanism. It also suggests that the degree of attenuation of seed-mediated OffT interactions is likely dependent on the siRNA sequence and the nature of the specific OffT interactions themselves.

DISCUSSION

The potential for hybridization-dependent siRNA OffT effects and subsequent risk for toxicity have been clear since the early days of the technology. Since then, preclinical studies have linked, for example, seed-mediated OffT effects with observed rodent toxicity.[35,36] To avoid this risk, *in-silico* predictions are often performed with highly permissive settings (i.e., with a large false positive rate) and then experimentally screened using untargeted methods like RNA-seq.[10] Here, we sought to expand our knowledge of possible biological mechanisms for potential hybridization-dependent siRNA OffT risk with the aim to refine *in-silico* predictions, reduce the risk of false positives, and help facilitate improved efficiency through the reduction of required experimental screening throughput.

By designing siRNAs with intentionally promiscuous OffT profiles, we were able to probe our assumptions about what a low-homology hybridization-dependent OffT may look like. Further, establishing and validating the catalytically inactive Ago2 D597A-expressing cell line allowed us to differentiate OffT interactions identified by untargeted experimental techniques as cleavage-dependent (at the stages of target cleavage and/or passenger strand cleavage, including siRNA-like and miRNA-like interactions) or cleavage-independent (i.e., seed-mediated and miRNA-like). Finally, comparing the OffT profiles of six siRNAs at both the mRNA and protein levels using untargeted experimental methods gave us insight into the transcript-to-protein translatability of the observed siRNA:OffT interactions.

Ago2 drives miRNA OffTs of fully ribose-modified siRNAs in a sequence-dependent manner

Here we show that OffT downregulation by siRNAs was reduced in A549 cells with catalytically inactive Ago2. This suggests that in the context of a fully ribose-modified, fully complementary siRNA duplex—a system characterized by high thermal stability—Ago2

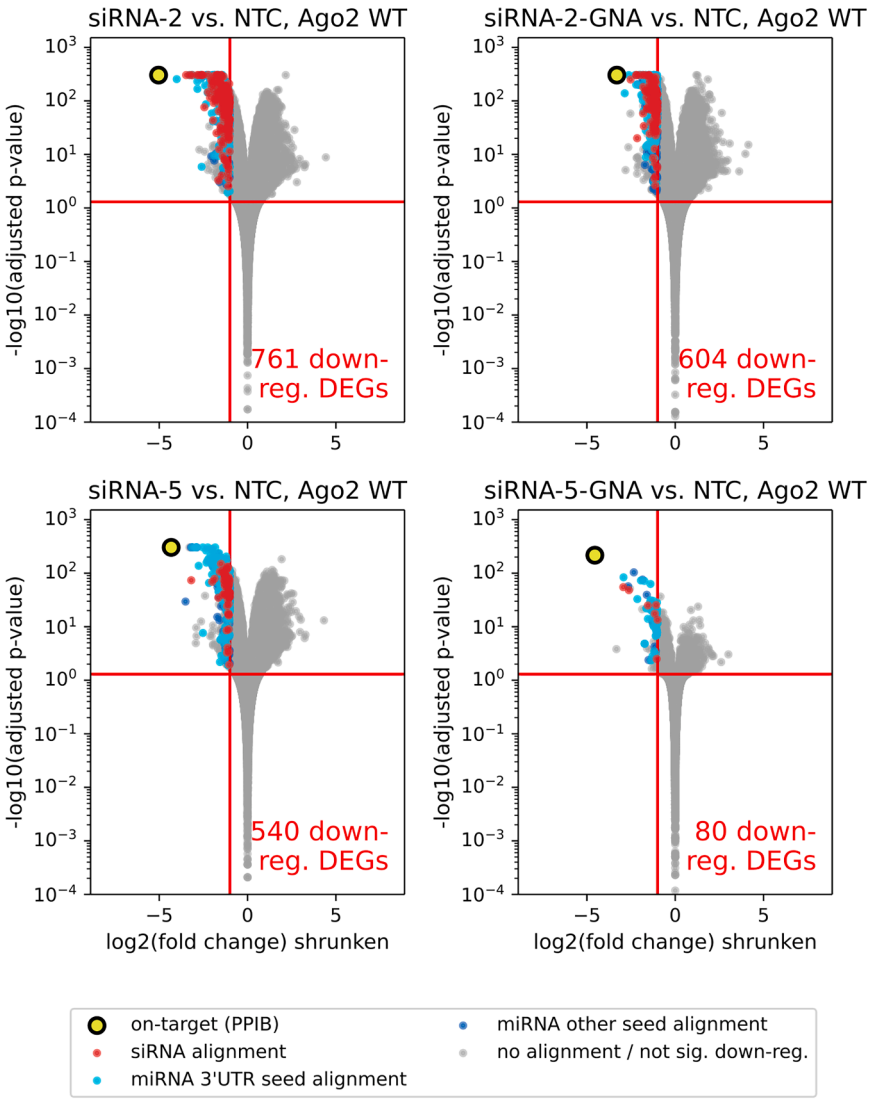

Figure 7. Effect of seed-destabilization chemistry on siRNA OffT profiles

siRNA-2 and siRNA-5 were synthesized with GNA included at specific positions within the seed shown to be compatible with on-target activity RNA-seq was performed after transfection with 20 nM of the siRNAs and incubation for 24 h and the fold-change relative to the NTC siRNA was calculated. Genes were considered significantly downregulated when the fold-change was ≤ 0.5 ($\geq 50\%$ downregulation) and the adjusted *p*-value was ≤ 0.05 (upper-left quadrant, red lines). The on-target (PPIB) is highlighted. Significantly downregulated genes are colored based on the IntaRNA alignment of the siRNA and the canonical transcript mRNA, red, siRNA-like alignment; light blue, 3′-UTR seed match; dark blue, non-3′-UTR seed match.

catalytic function may be required for both RISC maturation and target mRNA cleavage. It has been reported that LNA (locked nucleic acid)-modified siRNAs or siRNAs with high GC content show reduced OffT reporter activity in murine cells lacking Ago2; without the catalytic activity of Ago2, the unwinding of these duplexes is likely impaired in the remaining Ago proteins.[37] Similarly, enhanced Ago2 selectivity was demonstrated for two LNA-modified miRNAs with increased thermal stability, suggesting that loading of these siRNA guide strands was limited to catalytically active Ago2 and not other Ago proteins.[38] A recent rodent study also demonstrated that Ago2, but not Ago1, is involved in hepatotoxicity that can occur with a subset of GalNAc siRNA conjugates at exaggerated doses.[39]

In this study, we demonstrate that seed-mediated activity is impaired to different degrees in the six siRNA sequences characterized here (Figure S5). This could be affected by different siRNA asymmetries, i.e., a larger or smaller difference between local thermal stability in the guide 5′ and guide 3′ ends, and the unwinding behavior at the less thermally stable end. It may also be that a combination of nucleobase sequence and specific ribose modifications determines siRNA dependency on passenger strand cleavage vs. compatibility with a bypass mechanism that allows RISC maturation despite the lack of catalytic activity. Interestingly, this would also affect the susceptibility of different sequences being processed and loaded to active RISC in Ago1, Ago3, and Ago4, and would add an additional, sequence-dependent factor to the OffT risk arising from non-catalytic Ago family members. A previous study used stable overexpression of tagged, catalytically inactive Ago2, and subsequent SpyCLIP with unmodified siRNAs to identify both cleavage-dependent and -independent OffT sites for all siRNAs tested.[12] The thermal stability of the unmodified siRNA duplexes used in this previous study, however, is likely lower than a fully ribose-modified siRNA and therefore may be less dependent on catalytic Ago2 activity for RISC maturation.

Target bulges and multiple G:U wobbles are compatible with siRNA:OffT activity

By analyzing the global distribution of four different *in-silico* alignment features (mismatches, G:U wobbles, target bulges, and guide bulges) of both the siRNA:OffT interactions identified in this study and miRNA:target interactions reported in MiRTarBase several intriguing patterns emerge (Figure 5). Mismatches, for example, appear much more frequently at the 5′ and 3′ ends of the guide strand than in the central region of the sequence; a similar tolerance for mismatches at the 3′ end of the guide strand has been reported to not only be tolerated, but in some cases to also enhance the rate of target

cleavage.[5] Interestingly, mismatches are regularly found in the seed region in both the siRNA and miRNA alignments, suggesting that a perfect seed match is not strictly required to see OffT activity. Such a tolerance for low seed complementarity has been reported earlier, where SpyCLIP was used in cells stably expressing Ago2 D597A to identify cleaved siRNA OffT sites featuring both mismatches and bulges in the seed region.[12] G:U wobbles, in contrast, seem to be distributed relatively evenly across the guide sequence, although they are less frequently found at the cleavage site (positions g10 and g11).[5,27,28] It should be noted that the distribution of G:U wobbles seen here is inherently biased by the position of G's and U's in the six siRNAs tested, as G:U wobbles cannot, by definition, occur at other positions; however, in all six sequences tested here a G or U appears at least once in all 19 positions. Multiple mismatches and G:U wobbles are both apparently tolerated, with some alignments featuring a relatively large number of these edits.

Target bulges (i.e., insertions in the aligned target sequence) are found across the guide strand in this study, even within the seed, although multiple target bulges are not frequently seen. Surprisingly, some of these target bulges are relatively large (>3 nucleotides in length), which prompted us to validate and generalize a 5-nt target bulge interaction pattern using a luciferase reporter system (Figure 6). Guide bulges (i.e., insertions in the aligned guide sequence), by contrast, seem to be remarkably less represented, especially for the alignments classified here as siRNA-like. Although such bulges in fully ribose-modified siRNAs have been shown to be compatible with *in vivo* activity in a position-dependent manner, it may be that they are relatively less tolerated than target bulges in the context of endogenous OffTs.[40] This is in line with the structure of human Ago2, which pre-organizes the seed region in an A form helix.[41] In bacterial structures, guide strand bulges were demonstrated to distort this preformed helix, whereas target bulges are looped outward, thereby preserving RNA conformation and orientation of catalytic residues.[42]

The compatibility of any of these siRNA:OffT interaction patterns is likely to be sequence-dependent due to factors like GC content of both guide and target strands or target site accessibility in the OffT mRNA. Despite this, several trends emerge from this analysis that help inform potential improvements to assessing siRNA OffT risks based on *in-silico* alignments. First, the apparent tolerance of G:U wobbles in a relatively position-independent manner suggests these features should be treated differently than other types of mismatches. Second, target bulges are tolerated to a much higher degree than guide bulges, suggesting that *in-silico* alignments featuring the latter feature may be considered lower-risk. Finally, the comparison of fully chemically modified siRNA OffT interactions to those of endogenous miRNAs can, in some cases, be misleading, as features like guide bulges are highly tolerated in the latter but not the former.

Outlook

The qualitative analysis of the distribution of features found in *in-silico* alignments of the siRNA:OffT pairs identified in this study suggest that increasing the search space during siRNA OffT prediction may help better identify OffT risks. Introducing any new features into the alignment strategy, however, also comes with an increased risk of identifying false positives; the observations made in this study may help mitigate this effect by allowing certain features (e.g., guide bulges) to be down-prioritized, as they are apparently less compatible with siRNA-like OffT effects.

The sequence-dependent effect on sense strand unwinding and cleavage-independent activity seen in this study extends conclusions made from earlier observations.[39] While the thermodynamic stability of the fully ribose-modified siRNA clearly plays some role in the sequence dependence seen here, it is not enough to explain the observations in this study. Future experiments extending the sequence space and using the catalytically inactive Ago2 cell line described here would be enlightening. Further, using a method like immunoprecipitation and quantifying the amount of loaded siRNA guide strand in Ago2 or other Ago proteins would help confirm the hypothesis and bridge the connection between siRNA loading and apparent cleavage-independent OffT activity.

While the observations in this study can help mitigate the fundamental difficulties of predicting siRNA OffT risk through specific, targeted extensions to the alignment strategy (e.g., allowing position-specific target bulges but not guide bulges during *in-silico* alignment), there is no substitution for experimental screening of siRNA OffT risk in the target species using an untargeted method like RNA-seq.[10]

MATERIALS AND METHODS

In silico sequence design and siRNA:OffT alignment

Using proprietary software, 19mer siRNAs targeting PPIB were designed for optimal on-target knockdown activity. From these, a permissive (i.e., allowing multiple edits, including insertions/deletions) alignment-based OffT prediction was performed using the PaTMaN software (v.1.2.2)[43] aligning each 19mer sequence to human transcript cDNA sequences (Ensembl release 104). Six 19mer sequences were selected to maximize the number of aligned OffT transcripts (i.e., promiscuity) while retaining predicted on-target efficacy (discussed in more detail in the global transcript-level OffT profiles of promiscuous siRNAs by RNA-seq section).

Assessment of potential target sites of siRNA:OffT pairs identified by RNA-seq was performed using the IntaRNA software (v.3.4.1; Vienna RNA package 2.7.0 and boost 1.85.0) with default settings.[23–25] siRNA sequences were aligned to k-mers of length 50 with a step size of 25 of the Ensembl canonical transcript cDNA sequence (release 111); for each canonical transcript, the target site alignment with the lowest (i.e., most negative) predicted free energy was chosen as "best." Alignments between endogenous miRNAs and targets reported with "Functional MTI" in MiRTarBase (accessed 26.07.2025) were performed in the same manner.

Synthesis of oligonucleotides

All oligonucleotides were synthesized on an ÄKTA Oligopilot 10 or an LGC Mermade 48X synthesizer using standard phosphoramidite

chemistry. Standard methods provided by the synthesizer manufacturers were applied. For the synthesis of GalNAc-conjugated oligonucleotides previously published coupling procedures were used.[44]

X4 trebler amidite and GalNAc phosphoramidite building block (GN) were synthesized as previously described.[45]

Commercially available solid supports lcaa CpG 500 Å (loading ~50 μmol/g, standard protection ChemGenes) and 5′-DMT-2′-OMe and 5′-DMT-2′-F nucleotide phosphoramidites (all standard protection, Hongene Biotech), DMT-GNA-U phosphoramidites (WuXi TIDES) and DMT-C3-phosphoramidite (ChemGenes) were used according to the manufacturer's recommended procedures. Ancillary reagents were purchased from EMP Biotech and Biosolve. Oligonucleotide synthesis grade acetonitrile (<30 ppm H2O) was used as was synthesis wash and reagent diluent. Detritylation: 3% dichloroacetic acid in toluene, activator: 0.3 M benzylthiotetrazole (BTT) in ACN, capping: Ac_2O/NMI/Lutidine/Acetonitrile, Oxidizer: 0.1 M I_2 in pyridine/H_2O, sulfurization: 0.05 M (dimethylamino-methylidene) amino)-3H-1,2,4-dithiazoline-3-thione in pyridine (DDTT, Chemgenes). Upon completion of the programmed synthesis cycles, a diethylamine (DEA) wash was performed. All oligonucleotides were synthesized in DMT-off mode. The single strands were cleaved off the CpG by 40% aq. methylamine treatment.

Detailed description of purification, double strand formation, and oligonucleotide analysis are described in Schöllkopf et al.[44]

All other reagents and solvents were commercially available and used in standard reagent quality.

Oligonucleotide sequences, modification patterns, and analysis parameters are listed in Table S1.

Melting curve analysis

Melting curve experiments were performed on a Cary3500 (Agilent Technologies) ultraviolet-visible (UV-vis) spectrometer. Temperature ramp was set to 1 K per minute and the concentration was chosen to be at 0.5 absorption in the spectrometer in PBS buffer (Dulbecco's Phosphate Buffered Saline, MS01AM1007, BioWest). siRNA conjugates were placed in a quartz cuvette (Hellma HL114-10-40) with PBS buffer and the thermal heating/cooling cycle was applied three times. Any stated T_m values are the mean of three repeated measurements.

Ago2 editing in A549 cells

Two independent clones of A549 Ago2 D597A cells were obtained as fully edited and characterized from Synthego (Synthego, Redwood City, CA). Editing efficiency and quantification of generated indels was performed using interference of CRISPR edits (ICE) analysis (http://ice.synthego.com/). The used A549 WT cells were mock transfected. Genotyping results are shown in Figure S1.

Cell culture

A549 cells were cultured in F-12K Nut Mix medium (Gibco) with 10% fetal bovine serum (FBS) at 37°C and 5% CO_2.

siRNA transfection and RNA isolation

A549 cells were seeded at a density of 12,000 cells/well in 96-well format for TaqMan analysis or 150,000 cells/12-well for western blot analysis. Indicated concentration of siRNA were transfected using 0.3 μL Lipofectamin RNAiMaX (Thermo Fisher Scientific, Waltham, MA, USA) per well (96-well format) or 1.5 μL per well (12-well format) and added to the cells directly after seeding. Thereafter, cells were cultured at 37°C and 5% CO_2.

For RNA isolation the supernatant was discarded 24 h after treatment, cells were washed with PBS, and 250 μL of lysis buffer (Thermo Fisher Scientific, Waltham, MA, USA) was added. Plates were stored at −80°C until RNA isolation was performed on a King Fisher Flex system using Dynabeads mRNA direct Kit (both Thermo Fisher Scientific, Waltham, MA, USA).

RT-qPCR

For multiplex quantitative real-time PCR (quantitative real-time PCR [RT-qPCR], 0.5 U M-MLV reverse transcriptase (cat. #M368C; Promega, Madison, WI, USA), 5× master mix (UF-LP5X-C0510, Eurogentec, Seraing, Belgium) and primers and probes as indicated in Table S4 were used. RT-qPCR was performed in a 384-well plate with cDNA synthesis for 30 min at 48°C, 3 min initial denaturation at 95°C, and 40 cycles of 95°C for 10 s and 60°C for 60 s in a QuantStudio 6 RT cycler (Applied Biosystems, Waltham, MA, USA). Primers and probes were purchased from Eurofins Genomics (Ebersberg, Germany) or Eurogentec (Seraing, Belgium). Primer concentrations used for multiplex analysis are listed in Table S5.

Luciferase reporter system

Luciferase reporter plasmids were generated by cloning targeting sequences into the psiCHECK-2 vector (Promega, Fitchburg, WI, USA) between SgfI and PmeI restriction sites. The on-target reporter plasmid ("siRNA reporter") contained a single site with perfect complementarity to the guide strand in the 3′-UTR of Renilla luciferase. The OffT reporter plasmid ("miRNA reporter") contained four seed complementary sites separated by spacers in the 3′-UTR of Renilla luciferase.[46] Both plasmids co-expressed firefly luciferase as a transfection control. The specific insert sequences are listed in Table S6.

A549 WT and mutant cells were seeded at a density of 12,000 cells per well in 96-well format and co-transfected with the indicated concentration of siRNA and reporters during plating, using 0.3 μL/well Lipofectamin LTX and Plus reagent (Thermo Fisher Scientific, Waltham, MA, USA) and 50 ng/well (siRNA and miRNA reporters) or 5 ng/well (concatemer reporters). Dual-Glo® Luciferase Assay (Promega, Fitchburg, WI, USA) was performed 24 h after treatment or 48 h after treatment if specified.

Protein lysate and western blot analysis

Protein lysates for western blot analysis were prepared at the indicated time point using 150 µL 1× RIPA Buffer (9806s; Cell Signaling Technology) supplemented with 31.25 U/mL Benzonase (1.01654.001, Merck, Darmstadt, Germany) and 1× Protease inhibitor cocktail tablets (#12505200, Roche, Basel, Switzerland) after washing the cells with ice-cold PBS. The cells were incubated at 4°C for 30 min with gentle agitation. Lysate was collected in pre-cooled tubes and residual debris was removed by centrifugation.

Protein concentration was determined using BCA Assay (23225, Thermo Fisher Scientific, Waltham, MA, USA). Concentration of protein samples were adjusted and loaded at equal levels on 4%–20% gradient gel (Anamed, Groβ-Bieberau, Germany). After transfer, blots were incubated with primary antibodies diluted in Tris-buffered saline (TBS-T) and incubated overnight at 4°C with gentle agitation. Antibodies used in this study were Cyclophilin B (11607-1-AP; Proteintech, Planegg-Martinsried, Germany; dilution: 1:1,000) and PTEN (#9552S; Cell Signaling Technology, Danvers, USA; dilution 1:1,000). Secondary antibodies were diluted 1:40,000 in TBS and incubated 1 h at room temperature (Goat Anti-Rabbit IgG HRP (H + L) Cross-Adsorbed, G-21234, Thermo Fisher Scientific, Waltham, MA, USA). Imaging was done on a Jess automated western blot system (ProteinSimple, San Jose, USA).

RNA-seq and proteomics

For RNA-seq analysis 150,000 cells/well were seeded in a 12-well plate. 20 nM of siRNA was transfected using 3 µL Lipofectamin RNAiMaX (Thermo Fisher Scientific, Waltham, MA, USA) per well and added to the cells directly after seeding. Thereafter, cells were cultured at 37°C and 5% CO_2. After 24 h cells were washed with PBS and lysed using 250 µL lysis buffer (including a final concentration of 20 mM DTT) per well. RNA was isolated using NucleoSpin RNA Kit (740955.50, Machery&Nagel, Düren, Germany). RNA quality was analyzed with the 2100 Bioanalyzer System (Agilent Technologies, Santa Clara, CA, USA) using the RNA 6000 Nano Kit (Agilent Technologies, Santa Clara, CA, USA). RNA samples were stored at −80°C up to analysis. RNA-seq was performed by Novogene (Munich, Germany). After purifying mRNA from total RNA using poly-T oligo-attached magnetic beads, directional and non-directional libraries were prepared following standard protocols. The library was checked with Qubit and reverse-transcription PCR (RT-PCR) for quantification and bioanalyzer for size distribution detection. Quantified libraries were pooled and sequenced on Illumina platforms. Alignment to the human reference genome GRCh38.p14 was performed with HISAT2.[47] DGE analysis was performed using DESeq2 without independent filtering and a minimum of 10 reads; to calculate the log2(fold change), reads from samples treated with the promiscuous siRNAs were always compared to reads from samples treated with the NTC control.[48] All treated groups contained four replicates.

For label-free proteomics analysis 400,000 cells/well were seeded in a 6-well plate. 20 nM of siRNA were transfected using 16.8 µL Lipofectamin RNAiMaX (Thermo Fisher Scientific, Waltham, MA, USA) per well and added to the cells directly after seeding. Thereafter, cells were cultured at 37°C and 5% CO_2. Medium was removed after 24 h and fresh culture medium was added to the cells. Samples were collected 48 h after transfection. Therefore, the cells were washed twice with ice-cold PBS, scraped in cold PBS and centrifuged. The resulting pellets were snap frozen in liquid nitrogen. Cell pellets were stored at −80°C up to analysis. Proteomics analysis was performed by Biognosys (Schlieren, Switzerland). Samples were lysed and proteins were reduced and alkylated prior to tryptic digestion. The resulting peptides were purified via C18 columns before HRM liquid chromatography-tandem mass spectrometry (LC-MS/MS) protein profiling, targeted data extraction, and study-specific spectral library generation by directDIA+ search. Differential protein expression was performed using Biognosys' bioinformatic workflow, where samples treated with each promiscuous siRNA were compared to samples treated with the NTC siRNA. All treated groups contained four replicates.

DATA AND CODE AVAILABILITY

The authors confirm that the data supporting the findings of this study are available within the article and/or its supplemental information.

ACKNOWLEDGMENTS

We thank Gabi Anlauf, Jens Endruschat, Tino Struck, and Lucas Bethge for oligonucleotide synthesis, Nadja Demtschenko and Micaela Graglia for oligonucleotide analytics, and Justin Deim for performing *in vitro* experiments. All work in this study is sponsored by Silence Therapeutics with no additional funding or grants.

AUTHOR CONTRIBUTIONS

L.P.-D., J.H., N.W., M.W.L., and E.M. conceptualized the studies; L.P.-D., J.H., N.W. and E.M. designed experiments, analyzed the results, and prepared figures; V.H. performed experiments. All authors contributed to the writing of the manuscript.

DECLARATION OF INTERESTS

All authors are employees of and have stock options in Silence Therapeutics GmbH.

SUPPLEMENTAL INFORMATION

Supplemental information can be found online at https://doi.org/10.1016/j.omtn.2026.102972.

REFERENCES

1. Nakanishi, K. (2024). When Argonaute takes out the ribonuclease sword. J. Biol. Chem. *300*, 105499. https://doi.org/10.1016/j.jbc.2023.105499.

2. Selbach, M., Schwanhäusser, B., Thierfelder, N., Fang, Z., Khanin, R., and Rajewsky, N. (2008). Widespread changes in protein synthesis induced by microRNAs. Nature *455*, 58–63. https://doi.org/10.1038/nature07228.

3. Doench, J.G., Petersen, C.P., and Sharp, P.A. (2003). siRNAs can function as miRNAs. Genes Dev. *17*, 438–442. https://doi.org/10.1101/gad.1064703.

4. Doench, J.G., and Sharp, P.A. (2004). Specificity of microRNA target selection in translational repression. Genes Dev. *18*, 504–511. https://doi.org/10.1101/gad.1184404.

5. Becker, W.R., Ober-Reynolds, B., Jouravleva, K., Jolly, S.M., Zamore, P.D., and Greenleaf, W.J. (2019). High-Throughput Analysis Reveals Rules for Target RNA Binding and Cleavage by AGO2. Mol. Cell *75*, 741–755.e11. https://doi.org/10.1016/j.molcel.2019.06.012.

6. Wang, P.Y., and Bartel, D.P. (2024). The guide-RNA sequence dictates the slicing kinetics and conformational dynamics of the Argonaute silencing complex. Mol. Cell *84*, 2918–2934.e11. https://doi.org/10.1016/j.molcel.2024.06.026.

7. Jackson, A.L., Burchard, J., Schelter, J., Chau, B.N., Cleary, M., Lim, L., and Linsley, P.S. (2006). Widespread siRNA "off-target" transcript silencing mediated by seed region sequence complementarity. RNA *12*, 1179–1187. https://doi.org/10.1261/rna.25706.

8. Birmingham, A., Anderson, E.M., Reynolds, A., Ilsley-Tyree, D., Leake, D., Fedorov, Y., Baskerville, S., Maksimova, E., Robinson, K., Karpilow, J., et al. (2006). 3′ UTR seed matches, but not overall identity, are associated with RNAi off-targets. Nat. Methods *3*, 199–204. https://doi.org/10.1038/nmeth854.

9. Jackson, A.L., Bartz, S.R., Schelter, J., Kobayashi, S.V., Burchard, J., Mao, M., Li, B., Cavet, G., and Linsley, P.S. (2003). Expression profiling reveals off-target gene regulation by RNAi. Nat. Biotechnol. *21*, 635–637. https://doi.org/10.1038/nbt831.

10. Andersson, P., Burel, S.A., Estrella, H., Foy, J., Hagedorn, P.H., Harper, T.A., Henry, S.P., Hoflack, J.-C., Holgersen, E.M., Levin, A.A., et al. (2025). Assessing Hybridization-Dependent Off-Target Risk for Therapeutic Oligonucleotides: Updated Industry Recommendations. Nucleic Acid Therapeut. *35*, 16–33. https://doi.org/10.1089/nat.2024.0072.

11. Lindow, M., Vornlocher, H.-P., Riley, D., Kornbrust, D.J., Burchard, J., Whiteley, L.O., Kamens, J., Thompson, J.D., Nochur, S., Younis, H., et al. (2012). Assessing unintended hybridization-induced biological effects of oligonucleotides. Nat. Biotechnol. *30*, 920–923. https://doi.org/10.1038/nbt.2376.

12. Zhang, Y., Teng, Y., Xiao, W., Xu, B., Zhao, Y., Li, W., and Wu, L. (2020). Identifying Cleaved and Noncleaved Targets of Small Interfering RNAs and MicroRNAs in Mammalian Cells by SpyCLIP. Mol. Ther. Nucleic Acids *22*, 900–909. https://doi.org/10.1016/j.omtn.2020.10.009.

13. Liu, J., Carmell, M.A., Rivas, F.V., Marsden, C.G., Thomson, J.M., Song, J.-J., Hammond, S.M., Joshua-Tor, L., and Hannon, G.J. (2004). Argonaute2 Is the Catalytic Engine of Mammalian RNAi. Science *305*, 1437–1441. https://doi.org/10.1126/science.1102513.

14. Hauptmann, J., Schraivogel, D., Bruckmann, A., Manickavel, S., Jakob, L., Eichner, N., Pfaff, J., Urban, M., Sprunck, S., Hafner, M., et al. (2015). Biochemical isolation of Argonaute protein complexes by Ago-APP. Proc. Natl. Acad. Sci. *112*, 11841–11845. https://doi.org/10.1073/pnas.1506116112.

15. Grimm, D., Wang, L., Lee, J.S., Schürmann, N., Gu, S., Börner, K., Storm, T.A., and Kay, M.A. (2010). Argonaute proteins are key determinants of RNAi efficacy, toxicity, and persistence in the adult mouse liver. J. Clin. Investig. *120*, 3106–3119. https://doi.org/10.1172/jci43565.

16. Schmitter, D., Filkowski, J., Sewer, A., Pillai, R.S., Oakeley, E.J., Zavolan, M., Svoboda, P., and Filipowicz, W. (2006). Effects of Dicer and Argonaute down-regulation on mRNA levels in human HEK293 cells. Nucleic Acids Res. *34*, 4801–4815. https://doi.org/10.1093/nar/gkl646.

17. Yang, Y., and Mei, Q. (2020). Accumulation of AGO2 Facilitates Tumorigenesis of Human Hepatocellular Carcinoma. BioMed Res. Int. *2020*, 1631843. https://doi.org/10.1155/2020/1631843.

18. Garreau, M., Weidner, J., Hamilton, R., Kolosionek, E., Toki, N., Stavenhagen, K., Paris, C., Bonetti, A., Czechtizky, W., Gnerlich, F., and Rydzik, A. (2024). Chemical modification patterns for microRNA therapeutic mimics: a structure-activity relationship (SAR) case-study on miR-200c. Nucleic Acids Res. *52*, 2792–2807. gkae141. https://doi.org/10.1093/nar/gkae141.

19. Matranga, C., Tomari, Y., Shin, C., Bartel, D.P., and Zamore, P.D. (2005). Passenger-Strand Cleavage Facilitates Assembly of siRNA into Ago2-Containing RNAi Enzyme Complexes. Cell *123*, 607–620. https://doi.org/10.1016/j.cell.2005.08.044.

20. Rand, T.A., Petersen, S., Du, F., and Wang, X. (2005). Argonaute2 Cleaves the Anti-Guide Strand of siRNA during RISC Activation. Cell *123*, 621–629. https://doi.org/10.1016/j.cell.2005.10.020.

21. Leuschner, P.J.F., Ameres, S.L., Kueng, S., and Martinez, J. (2006). Cleavage of the siRNA passenger strand during RISC assembly in human cells. EMBO Rep. *7*, 314–320. https://doi.org/10.1038/sj.embor.7400637.

22. Kanzaki, H., Ito, S., Hanafusa, H., Jitsumori, Y., Tamaru, S., Shimizu, K., and Ouchida, M. (2011). Identification of direct targets for the miR-17-92 cluster by proteomic analysis. Proteomics *11*, 3531–3539. https://doi.org/10.1002/pmic.201000501.

23. Mann, M., Wright, P.R., and Backofen, R. (2017). IntaRNA 2.0: enhanced and customizable prediction of RNA–RNA interactions. Nucleic Acids Res. *45*, W435–W439. https://doi.org/10.1093/nar/gkx279.

24. Wright, P.R., Georg, J., Mann, M., Sorescu, D.A., Richter, A.S., Lott, S., Kleinkauf, R., Hess, W.R., and Backofen, R. (2014). CopraRNA and IntaRNA: predicting small RNA targets, networks and interaction domains. Nucleic Acids Res. *42*, W119–W123. https://doi.org/10.1093/nar/gku359.

25. Busch, A., Richter, A.S., and Backofen, R. (2008). IntaRNA: efficient prediction of bacterial sRNA targets incorporating target site accessibility and seed regions. Bioinformatics *24*, 2849–2856. https://doi.org/10.1093/bioinformatics/btn544.

26. Raden, M., Ali, S.M., Alkhnbashi, O.S., Busch, A., Costa, F., Davis, J.A., Eggenhofer, F., Gelhausen, R., Georg, J., Heyne, S., et al. (2018). Freiburg RNA tools: a central online resource for RNA-focused research and teaching. Nucleic Acids Res. *46*, W25–W29. https://doi.org/10.1093/nar/gky329.

27. Elbashir, S.M., Martinez, J., Patkaniowska, A., Lendeckel, W., and Tuschl, T. (2001). Functional anatomy of siRNAs for mediating efficient RNAi in Drosophila melanogaster embryo lysate. EMBO J. *20*, 6877–6888. https://doi.org/10.1093/emboj/20.23.6877.

28. Sheu-Gruttadauria, J., Pawlica, P., Klum, S.M., Wang, S., Yario, T.A., Schirle Oakdale, N.T., Steitz, J.A., and MacRae, I.J. (2019). Structural Basis for Target-Directed MicroRNA Degradation. Mol. Cell *75*, 1243–1255.e7. https://doi.org/10.1016/j.molcel.2019.06.019.

29. Schnall-Levin, M., Zhao, Y., Perrimon, N., and Berger, B. (2010). Conserved microRNA targeting in Drosophila is as widespread in coding regions as in 3′UTRs. Proc. Natl. Acad. Sci. *107*, 15751–15756. https://doi.org/10.1073/pnas.1006172107.

30. Moretti, F., Thermann, R., and Hentze, M.W. (2010). Mechanism of translational regulation by miR-2 from sites in the 5′ untranslated region or the open reading frame. RNA *16*, 2493–2502. https://doi.org/10.1261/rna.2384610.

31. Huang, H.-Y., Lin, Y.-C.-D., Li, J., Huang, K.-Y., Shrestha, S., Hong, H.-C., Tang, Y., Chen, Y.-G., Jin, C.-N., Yu, Y., et al. (2020). miRTarBase 2020: updates to the experimentally validated microRNA–target interaction database. Nucleic Acids Res. *48*, D148–D154. https://doi.org/10.1093/nar/gkz896.

32. Cui, S., Yu, S., Huang, H.-Y., Lin, Y.-C.-D., Huang, Y., Zhang, B., Xiao, J., Zuo, H., Wang, J., Li, Z., et al. (2025). miRTarBase 2025: updates to the collection of experimentally validated microRNA–target interactions. Nucleic Acids Res. *53*, D147–D156. https://doi.org/10.1093/nar/gkae1072.

33. Huang, H.-Y., Lin, Y.-C.-D., Cui, S., Huang, Y., Tang, Y., Xu, J., Bao, J., Li, Y., Wen, J., Zuo, H., et al. (2022). miRTarBase update 2022: an informative resource for experimentally validated miRNA–target interactions. Nucleic Acids Res. *50*, D222–D230. https://doi.org/10.1093/nar/gkab1079.

34. Schlegel, M.K., Janas, M.M., Jiang, Y., Barry, J.D., Davis, W., Agarwal, S., Berman, D., Brown, C.R., Castoreno, A., LeBlanc, S., et al. (2022). From bench to bedside: Improving the clinical safety of GalNAc–siRNA conjugates using seed-pairing destabilization. Nucleic Acids Res. *50*, 6656–6670. https://doi.org/10.1093/nar/gkac539.

35. Jackson, A.L., and Linsley, P.S. (2010). Recognizing and avoiding siRNA off-target effects for target identification and therapeutic application. Nat. Rev. Drug Discov. *9*, 57–67. https://doi.org/10.1038/nrd3010.

36. Janas, M.M., Schlegel, M.K., Harbison, C.E., Yilmaz, V.O., Jiang, Y., Parmar, R., Zlatev, I., Castoreno, A., Xu, H., Shulga-Morskaya, S., et al. (2018). Selection of GalNAc-conjugated siRNAs with limited off-target-driven rat hepatotoxicity. Nat. Commun. *9*, 723. https://doi.org/10.1038/s41467-018-02989-4.

37. Petri, S., Dueck, A., Lehmann, G., Putz, N., Rüdel, S., Kremmer, E., and Meister, G. (2011). Increased siRNA duplex stability correlates with reduced off-target and elevated on-target effects. RNA *17*, 737–749. https://doi.org/10.1261/rna.2348111.

38. Ma, H., Zhang, J., and Wu, H. (2014). Designing Ago2-specific siRNA/shRNA to Avoid Competition with Endogenous miRNAs. Mol. Ther. Nucleic Acids *3*, e176. https://doi.org/10.1038/mtna.2014.27.

39. Agarwal, S., Taft, E., Gauthier, M., Darcy, J., Buckowing, K., Berman, D., Davis, W.P., Rogers, A.B., and Janas, M.M. (2025). Mechanistic Insights into Hybridization-Based

On-Target Activity of GalNAc-siRNA Conjugates. Nucleic Acid Therapeut. *35*, 125–136. https://doi.org/10.1089/nat.2024.0090.

40. Hauptmann, J., Hehne, V., Balzer, M., Bethge, L., and Wikstrom Lindholm, M. (2022). Engineering miRNA features into siRNAs: Guide-strand bulges are compatible with gene repression. Mol. Ther. Nucleic Acids *27*, 1116–1126. https://doi.org/10.1016/j.omtn.2022.02.004.
41. Schirle, N.T., Sheu-Gruttadauria, J., and MacRae, I.J. (2014). Structural basis for microRNA targeting. Science *346*, 608–613. https://doi.org/10.1126/science.1258040.
42. Sheng, G., Gogakos, T., Wang, J., Zhao, H., Serganov, A., Juranek, S., Tuschl, T., Patel, D.J., and Wang, Y. (2017). Structure/cleavage-based insights into helical perturbations at bulge sites within T. thermophilus Argonaute silencing complexes. Nucleic Acids Res. *45*, 9149–9163. https://doi.org/10.1093/nar/gkx547.
43. Prüfer, K., Stenzel, U., Dannemann, M., Green, R.E., Lachmann, M., and Kelso, J. (2008). PatMaN: rapid alignment of short sequences to large databases. Bioinformatics *24*, 1530–1531. https://doi.org/10.1093/bioinformatics/btn223.
44. Schöllkopf, S., Rathjen, S., Graglia, M., Was, N., Morrison, E., Weingärtner, A., Bethge, L., Hauptmann, J., and Wikström Lindholm, M. (2024). The beauty of symmetry: siRNA phosphorodithioate modifications reduce stereocomplexity, ease analysis, and can improve in vivo potency. Mol. Ther. Nucleic Acids *35*, 102336. https://doi.org/10.1016/j.omtn.2024.102336.
45. Frauendorf, C., and Cameron, M. (2017). Nucleic Acid Linked to a Trivalent Glycoconjugate. WO2017174657A1.
46. Sætrom, P., Heale, B.S.E., Snøve, O., Aagaard, L., Alluin, J., and Rossi, J.J. (2007). Distance constraints between microRNA target sites dictate efficacy and cooperativity. Nucleic Acids Res. *35*, 2333–2342. https://doi.org/10.1093/nar/gkm133.
47. Mortazavi, A., Williams, B.A., McCue, K., Schaeffer, L., and Wold, B. (2008). Mapping and quantifying mammalian transcriptomes by RNA-Seq. Nat. Methods *5*, 621–628. https://doi.org/10.1038/nmeth.1226.
48. Love, M.I., Huber, W., and Anders, S. (2014). Moderated estimation of fold change and dispersion for RNA-seq data with DESeq2. Genome Biol. *15*, 550. https://doi.org/10.1186/s13059-014-0550-8.